⌘ *Author's Choice*

RIC-3 Exclusively Enhances the Surface Expression of Human Homomeric 5-Hydroxytryptamine Type 3A (5-HT$_3$A) Receptors Despite Direct Interactions with 5-HT3A, -C, -D, and -E Subunits*[S]

Jutta Walstab[‡§], **Christian Hammer**[‡], **Felix Lasitschka**[¶], **Dorothee Möller**[‡], **Christopher N. Connolly**[‖],
Gudrun Rappold[‡], **Michael Brüss**[§], **Heinz Bönisch**[§], and **Beate Niesler**[‡1]

From the ‡*Department of Human Molecular Genetics, University of Heidelberg, Im Neuenheimer Feld 366, 69120 Heidelberg, Germany,* §*Institute of Pharmacology and Toxicology, University of Bonn, Reuterstrasse 2b, 53113 Bonn, Germany,* ¶*Institute of Pathology, University of Heidelberg, Im Neuenheimer Feld 220/221, 69120 Heidelberg, Germany, and* ‖*Centre for Neuroscience, Division of Medical Sciences, Ninewells Medical School, University of Dundee, Dundee DD1 9SY, Scotland, United Kingdom*

Although five 5-hydroxytryptamine type 3 (5-HT3) subunits (A–E) have been cloned, knowledge on the regulation of their assembly is limited. RIC-3 has been identified as a chaperone specific for the pentameric ligand-gated nicotinic acetylcholine and 5-HT$_3$ receptors. Therefore, we examined the impact of RIC-3 on differently composed 5-HT$_3$ receptors with the focus on 5-HT3C, -D, and -E subunits. The influence of RIC-3 on these receptor subtypes is supported by the presence of *RIC3* mRNA in tissues expressing at least one of the subunits 5-HT3C, -D, and -E. Furthermore, immunocytochemical studies on transfected mammalian cells revealed co-localization in the endoplasmic reticulum and direct interaction of RIC-3 with 5-HT3A, -C, -D, and -E. Functional and pharmacological characterization was performed using HEK293 cells expressing 5-HT3A or 5-HT3A + 5-HT3B (or -C, -D, or -E) in the presence or absence of RIC-3. Ca^{2+} influx analyses revealed that RIC-3 does not influence the 5-HT concentration-response relationship on 5-HT$_3$A receptors but leads to differential increases of 5-HT-induced maximum response (E_{max}) on cells expressing different subunits. Increases of E_{max} were due to analogously enhanced B_{max} values for binding of the 5-HT$_3$ receptor antagonist [^{3}H]GR65630. The observed enhanced cell surface expression of the tested 5-HT3 subunit combinations correlated with the increased surface expression of 5-HT3A as determined by flow cytometry. In conclusion, we showed that RIC-3 can interact with 5-HT3A, -C, -D, and -E subunits and predominantly enhances the surface expression of homomeric 5-HT$_3$A receptors in HEK293 cells. These data implicate a possible role of RIC-3 in determining 5-HT$_3$ receptor composition *in vivo*.

Cell surface proteins are translocated to the endoplasmic reticulum (ER)[2] of eukaryotic cells during synthesis. Thereby, posttranslational covalent modifications such as *N*-glycosylation and disulfide bond formation occur within the ER during the folding of the polypeptide. The assembly and trafficking of newly translated polypeptides are achieved with the help of chaperones. Many receptor-interacting proteins, which are involved in the trafficking and clustering of ligand-gated ion channels (LGICs), have already been identified (1). The assembly of the subunits in the ER is the rate-limiting step in the biogenesis of oligomeric LGICs (2). The ER-resident chaperones immunoglobulin heavy chain-binding protein (BiP) and calnexin have been shown to participate in subunit assembly of LGICs such as nicotinic acetylcholine (nACh) receptors (3–5) and 5-hydroxytryptamine type 3 (5-HT$_3$) receptors (6). In addition to these generalized chaperones, much more selective proteins such as stargazin for α-amino-3-hydroxy-5-methylisoxazole-4-proprionic acid receptors (AMPA) (7), 14-3-3η for nACh receptors (8), and RIC-3 for nACh and 5-HT$_3$ receptors (9) have been found. The latter has been identified in *Caenorhabditis elegans* as a protein involved in cholinergic signaling (10). It has been shown to enhance the surface expression of various nACh receptor subtypes (11–15) and of homomeric 5-HT$_3$A receptors (16), probably through an interaction with unassembled subunits in the ER (16, 17), whereas the two other members of the superfamily of Cys-loop LGIC, *i.e.* γ-aminobutyric acid type A and glycine receptors, seem to be unaffected by RIC-3 (11, 12, 14, 17).

Like all other Cys-loop LGICs, 5-HT$_3$ receptors are oligomeric complexes composed of five subunits. They exhibit a central role in the bidirectional brain-gut axis, which represents the neuronal connection between the enteric and the central nerv-

---

⌘ *Author's Choice*—Final version full access.
[S] The on-line version of this article (available at http://www.jbc.org) contains supplemental Figs. 1 and 2 and Tables 1 and 2.
[1] To whom correspondence should be addressed: Inst. of Human Genetics, Dept. of Human Molecular Genetics, Im Neuenheimer Feld 366, 69120 Heidelberg, Germany. Tel.: 49-6221-565058; Fax: 49-6221-568884; E-mail: beate.niesler@med.uni-heidelberg.de.

---

[2] The abbreviations used are: ER, endoplasmic reticulum; LGIC, ligand-gated ion channel; BiP, immunoglobulin heavy chain-binding protein; nACh, nicotinic acetylcholine; RIC-3, resistant to inhibitors of choline esterase type 3; FI, fluorescence index; pEC$_{50}$, $-\log_{10}$ of half-effective concentration; E_{max}, maximum response; B_{max}, maximum binding capacity; K_d, dissociation constant; 5-HT, 5-hydroxytryptamine; HA, hemagglutinin; HEK, human embryonic kidney; PBS, phosphate-buffered saline; Bis-Tris, 2-[bis(2-hydroxyethyl)amino]-2-(hydroxymethyl)propane-1,3-diol; FACS, fluorescence-activated cell sorting; RLU, relative light units.

ous system via the vagus nerve and mediates the regulation of digestion, emotions, and cognition. Consequently, besides their well established role in chemo-/radiotherapy-induced nausea and vomiting, 5-HT₃ receptors are involved in the pathophysiology of neurogastrointestinal and neuropsychiatric disorders (44). To date, five 5-HT3 subunits have been cloned from human: 5-HT3A, -B, -C, -D, and -E (19–23). The 5-HT3A subunit is able to form functional homomeric receptors, whereas the other subunits are only functional when co-expressed with 5-HT3A. Because these subunits are co-expressed in various tissues, *e.g.* the gastrointestinal tract (23, 24), specific mechanisms must exist that determine receptor composition, which in turn defines the properties of 5-HT₃ receptors. Limited information is available regarding these mechanisms and factors involved. However, some chaperone molecules have been shown to be involved in determining subunit composition of LGICs. The protein 14-3-3η has been reported to alter the stoichiometry of α4β2 nACh receptors (25), and there is first evidence that RIC-3 plays a role in determining subunit composition of nACh and 5-HT₃ receptors. 1) It has been shown to promote the expression of homomeric 5-HT₃A at the expense of heteromeric 5-HT₃AB receptors in mammalian cells (17), and 2) it leads to a preferential expression of DEG-3-rich DEG-3/DES-2 nACh receptors in *C. elegans* (26, 27).

The major aim of this study was to investigate the impact of the specific chaperone RIC-3 on 5-HT₃ receptors of various compositions. Given that the interaction of BiP and calnexin with 5-HT₃A and 5-HT₃AB receptors is known (6), another aim of this study was to determine whether these generalized chaperones also monitor the folding and assembly of 5-HT₃ receptors containing the human subunits 5-HT3C, -D, and -E. This may help to elucidate the mechanism of how homomeric, as well as heteromeric, 5-HT₃ receptor formation is regulated *in vivo* and may provide a first step toward the development of more selective compounds for the treatment of neurogastrointestinal and neuropsychiatric disorders.

MATERIALS AND METHODS

Chemicals and Drugs—Coelenterazine *h* was from Nanolight (Pinetop, AZ). 5-HT creatinine sulfate (serotonin) was obtained from Sigma. [³H]GR65630 (3-(5-[³H]methyl-1*H*-imidazol-4-yl)-1-(1-methyl-1*H*-indol-3-yl)-1-propanone; specific activity, 76.4 Ci/mmol) was from PerkinElmer Life Sciences.

Expression Constructs—The human 5-HT3A, -B, -C, -D, -E, and -Ea subunit-encoding cDNAs from *HTR3A, -B, -C, -D, -E,* and *-Ea* (Table 1) were cloned into the expression vector pcDNA3 (Invitrogen). To enable detection of the encoded proteins in flow cytometry or glycosylation experiments, Myc and/or HA epitope tags were introduced within the extracellularly located N terminus of the subunits (see Ref. 28). The apoaequorin cDNA (GenBank™ accession number L29571), originally derived from cytAEQ/pcDNA1 (Molecular Probes-Invitrogen), was subcloned into HindIII/XbaI-digested pcDNA3.1/zeo(+) (Invitrogen). Oligonucleotide primers based on the human *RIC3* sequence (GenBank accession number NM_024557; sense, GACCACCGTGAGCAGTCATG; antisense, GAGGAGAGAGAGGTCACCTTG) were used to amplify *RIC3*

TABLE 1

Primer sequences for expression analysis by reverse transcription-PCR

Gene/primer[a]	Sequence (5′ → 3′)	Amplicon size	GenBank accession no.
		bp	
HTR3A		159	AJ003079
for	CCTGGTTCTGGAGAGAATCG		
rev	GGGCTCTTCTCGAAGTCCTG		
HTR3C		418	AF459285
for	TCCCCAGAGAAGAGTCCAGA		
rev	TGGATTCCACGATGAAGATG		
HTR3D		624	AY159812
for	CTGGTGACATCGTTCCTGTG		
rev	TGGGAGCAAGTCATTCATCA		
HTR3E		524	AY159813 (E)
for	ATGTTAGCTTTCATTTTATCACGGGC		DQ644022 (Ea)
rev	CTGTCCACCTTCATGGGTTT		
RIC3		1180	NM_024557
for	GACCACCGTGAGCAGTCATG		
rev	GAGGAGAGAGAGGTCACCTTG		
ARF		336	NM_001024227.1
for	GCCAGTGTCCTTCCACCTGTC		
rev	GCCTCGTTCACACGCTCTCTG		

[a] for, forward; rev, reverse; ARF, ADP-ribosylation factor.

cDNA from human liver cDNA. The resulting fragment was subcloned into pCR2.1 (Invitrogen), excised with HindIII/EcoRI, and subcloned into pcDNA3.1(−). The fidelity of the cDNA sequences was verified by sequencing.

Expression Analysis—RNAs from 14 different human adult tissues (Clontech) were reverse transcribed using the Superscript III First-Strand Synthesis System (Invitrogen) as designed by the manufacturer. PCR analysis was performed using different gene-specific primers (Table 1). Reaction mixtures of 25 μl contained 10–100 ng of template, 25 pmol of each primer, 200 μM dNTPs (MBI Fermentas, St. Leon-Roth, Germany), 1.5 mM MgCl₂, 1× PCR buffer, and 2 units of HotStarTaq DNA polymerase (Qiagen, Hilden, Germany). Thermal cycling was performed as follows: initial denaturation at 94 °C for 15 min followed by 35–40 cycles of 94 °C for 30 s, 60 °C for 30 s, and 72 °C for 2 min. Final extension was carried out at 72 °C for 5 min.

Cell Culture and Transfection—Human embryonic kidney (HEK) 293 and human osteosarcoma U2OS cells (ATCC, Manassas, VA) were grown as monolayers in Dulbecco's modified Eagle's medium/Ham's F-12 (1:1) supplemented with 10% fetal calf serum, 100 units/ml penicillin, and 100 μg/ml streptomycin in a humidified atmosphere containing 5% CO₂ at 37 °C. Transient transfection was performed with Polyfect transfection reagent (Qiagen) according to the manufacturer's instructions. For immunocytochemical experiments and radioligand binding, the following mixtures of cDNAs were used: (*a*) single subunits (5-HT3A, -B, -C, -D, and -Ea): 20% 5-HT3 subunit cDNA and 80% pcDNA3; and (*b*) co-expression of 5-HT3A with 5-HT3B (or -C, -D, -E, or -Ea): 20% 5-HT3A and 80% 5-HT3B (or -C, -D, -E, or -Ea) cDNA (1:4 ratio to promote the formation of heteromeric receptors). For immunofluorescence and flow cytometry experiments, Myc- or HA-tagged subunit constructs were used. For aequorin assays, cDNA amounts used were as follows: (*a*) homomeric 5-HT₃A receptors: 67% apoaequorin cDNA and 33% 5-HT3A cDNA and pcDNA3 combination (1:4); and (*b*) co-expression of 5-HT3A with 5-HT3B (or -C, -D, -E, or -Ea): 67% apoaequorin cDNA and 33%

5-HT3A and 5-HT3B (or -C, -D, -E, or -Ea) cDNA combination (1:4). For expression of RIC-3, $\frac{1}{10}$ RIC-3 cDNA (related to the total 5-HT3 subunit cDNA amount) was included unless otherwise indicated.

Immunofluorescence Experiments—HEK293 and U2OS cells, seeded on poly-L-lysine-coated coverslips in 12-well plates, were transfected using a total amount of 1 μg of DNA/well. Cells were analyzed 24 h after transfection. Briefly, cells were washed twice using 1× phosphate-buffered saline (PBS) and fixed by incubation in 3.75% paraformaldehyde for 15 min. Afterward, they were washed 3 × 5 min in 1× PBS at room temperature and then permeabilized in 0.1% Triton X-100, PBS. The primary antibodies mouse anti-Myc (Cell Signaling Technology, 9B11), mouse anti-HA (Sigma, HA-7), and sheep anti-RIC-3, diluted in 1× PBS, were applied for 1 h at room temperature. Cells were washed 3 × 5 min in 1× PBS and incubated with the fluorochrome-labeled secondary antibodies (anti-mouse/sheep Alexa Fluor 488 (Invitrogen)) in 1× PBS for 1 h. From this point on, every step was carried out light-protected. Cells were washed 3 × 5 min in 1× PBS. A nuclear counterstain with 4′,6-diamidino-2-phenylindole (1:10,000) was carried out. Then cells were washed twice in 1× PBS at room temperature and mounted in Mowiol (Calbiochem, Merck). The slides were stored at 4 °C until microscopic examination. Microscopy was performed with a Zeiss Axiophot system, and images were taken and analyzed using the Leica FW4000 application (Leica, Nussloch, Germany).

Co-immunoprecipitation—HEK293 cells, seeded in 6-cm cell culture dishes coated with poly-L-lysine, were transfected with a total amount of 10 μg of DNA/dish. Twenty-four hours following transfection cells were L-methionine-starved for 30 min before being labeled with [^{35}S]methionine/cysteine (0.2 mCi/dish; Hartmann Analytic, Braunschweig, Germany) for 24 h. Cells were lysed in a 10 mM sodium phosphate-based lysis buffer (6) for 1 h on ice. After centrifugation (16,000 × g for 10 min), the supernatant was incubated with 10 μl of UltraLink Immobilized Protein A/G resin (Thermo Fisher Scientific Inc., Rockwell, IL) for 16 h at 4 °C to remove nonspecific binding. After centrifugation (16,000 × g for 5 min), the supernatant was split and incubated with either 5 μl of the respective 5-HT3 subunit- or chaperone-specific antibody for 24 h at 4 °C. After 6 h, 5 μl of the UltraLink resin were added. The resin was washed three times with a 10 mM sodium phosphate-based buffer containing 5 mM EDTA, 5 mM EGTA, 50 mM NaF, 50 mM NaCl, and 1 mM sodium orthovanadate. Analysis was performed using SDS-polyacrylamide gel electrophoresis with NuPAGE 4–12% Bis-Tris gels (Invitrogen) followed by vacuum drying and autoradiography on BioMax films (Eastman Kodak Co.) at −80 °C.

Site-directed Mutagenesis for Glycosylation Studies—According to the technique of gene splicing by overlap extension (29, 30), mutated 5-HT3Ea constructs with specific nucleotide exchanges affecting the predicted *N*-glycosylation sites were created by two-step polymerase chain reaction with flanking primers and internal primers carrying the desired mutation. Mutagenesis of 5-HT3C was performed using the QuikChange Lightning site-directed mutagenesis kit (Stratagene, La Jolla, CA). The primers used are listed in supplemental Table 1.

Tunicamycin Treatment of HEK293 Cells—Twenty-four hours posttransfection, HEK293 cells were incubated with 5 μg/ml tunicamycin for 24 h to block *N*-linked glycosylation.

Western Blotting—Transfected cells were harvested 48 h posttransfection and incubated in 300 μl of lysis buffer (6) for 1 h on ice. Total protein was determined using the BCA Protein Assay kit (Pierce), and 10 μg of protein were loaded on 4–12% Bis-Tris NuPAGE gels (Invitrogen). Gels were blotted onto polyvinylidene difluoride membranes using the XCell system (Invitrogen). Detection was accomplished following the "Odyssey Western Blot Analysis" protocol (Li-Cor Biosciences, Lincoln, NE). The primary antibodies anti-5-HT3C and anti-5-HT3D/E (supplemental Table 2) were diluted 1:500; secondary antibody (donkey anti-rabbit IRDye 680, Li-Cor Biosciences) was diluted 1:10,000.

Radioligand Binding Assay—HEK293 cells, seeded in 75-cm^2 culture flasks, were transfected with a total amount of 15 μg of cDNA/flask. Preparation of membranes and [^{3}H]GR65630 binding was carried out 48 h later as described previously (28, 30). For saturation experiments, 4 μg of membranes were incubated in duplicates with five increasing concentrations (0.02–1.5 nM) of [^{3}H]GR65630 for 1 h. Nonspecific binding was determined on mock-transfected cells. Incubation mixtures were filtered through GF/B filters, presoaked with 0.5% polyethylenimine, using a Brandel cell harvester followed by three washes with ice-cold buffer. Radioactivity was measured in a liquid scintillation counter (Beckman Coulter, Fullerton, CA).

Aequorin Luminescence-based Ca^{2+} Influx Assay—HEK293 cells, seeded in 25- or 75-cm^2 culture flasks, were transfected with a total amount of 5 or 15 μg of cDNA/flask, respectively. The aequorin assay was performed 48 h later as described previously (31). Harvested cells were loaded with 5 μM coelenterazine *h* for 2.5 h at room temperature. Suspensions of cells in assay buffer were used for luminometric determination of intracellular Ca^{2+} transients in 96-well plates in a Centro LB 960 luminometer (Berthold, Bad Wildbad, Germany). Luminescence was recorded 5 s prior and 15–60 s upon autoinjection of 5-HT at a sampling rate of 2 Hz. At the end of the experiments in which 5-HT maximum responses were recorded, cells were lysed by autoinjection of 0.1% Triton X-100 (v/v), 50 mM CaCl$_2$, and remaining aequorin luminescence was recorded to obtain the maximum possible Ca^{2+} response.

Flow Cytometry—HEK293 cells, seeded in 12-well plates, were transfected with a total amount of 0.75 μg of cDNA/well. Forty-eight hours following transfection, cells were harvested after treatment with Accutase (PAA Laboratories, Pasching, Austria) and washed with PBS. Cells expressing HA- and Myc-tagged 5-HT3 subunits were incubated with mouse anti-HA or mouse anti-Myc antibody (supplemental Table 2) for 1 h on ice. After washing the cells with PBS, they were incubated with the secondary Alexa Fluor 488 anti-mouse antibody (supplemental Table 2) for 20 min on ice. Following a washing step with PBS, cells were resuspended in 150 μl of FACS buffer (BD Perm/Wash, BD Biosciences). Samples were run on a FACSCalibur system (BD Biosciences). For each staining condition, 30,000

cells were analyzed using CellQuest Pro 4.0.2 software (BD Biosciences). Cells with a mean fluorescence intensity (MFI) >99% of mock-transfected cells were defined as positive. Data are presented as "fluorescence indices" (FIs) as has been previously done for γ-aminobutyric acid type A receptors: FI = percentage of positive cells × MFI (32).

*Data Analysis*—Relative light units (RLU) for increases of the intracellular Ca^{2+} concentration, measured as aequorin luminescence, were obtained by subtraction of baseline luminescence from the 5-HT-induced peak luminescence. In 5-HT maximum response experiments, the peak luminescence (RLU_{peak}) was normalized against total aequorin luminescence (RLU_{max}) after cell lysis to control for differences in transfection efficiency and cell number ($RLU_{peak}/(RLU_{peak} + RLU_{max})$). The concentration-response curves and saturation binding curves as well as the pEC_{50} values, Hill slopes, and binding constants maximum binding capacity (B_{max}) and K_d were calculated by means of GraphPad Prism 5.0 (GraphPad Software Inc., San Diego, CA). Data are given as means ± S.E. Statistical analysis was performed with unpaired Student's *t* test or one-way analysis of variance followed by Dunnett's or Tukey's post hoc test. Differences were considered significant at $p < 0.05$.
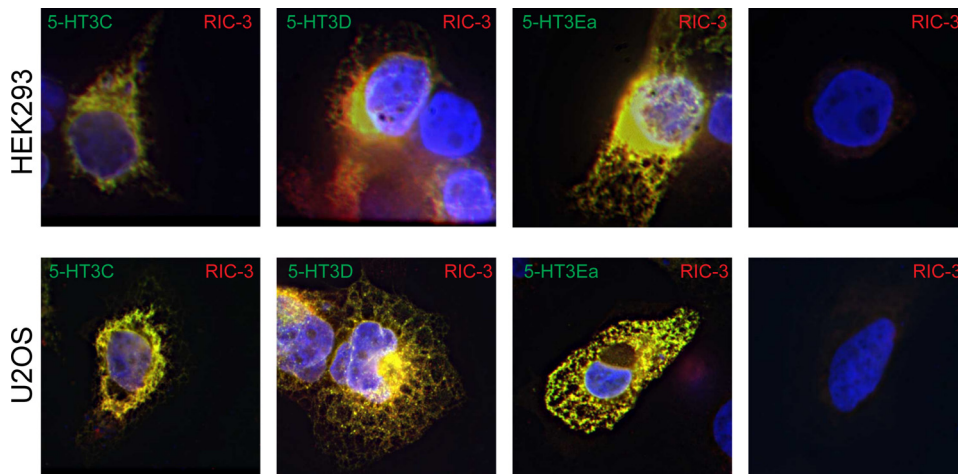
RESULTS

Co-expression of RIC-3 and 5-HT3C, -D, and -E

We performed comparative expression analysis by reverse transcription-PCR, amplifying parts of the coding regions of the genes *HTR3A*, *-C*, *-D*, and *-E* and the complete coding region of *RIC3* using 14 cDNAs prepared from human adult tissues (Fig. 1). *HTR3C* and *HTR3D* presented with different splice forms corresponding to isoforms that were described recently (33). In line with previous data, transcription of *HTR3A* and *HTR3C* was ubiquitous, and for *HTR3D*, highest expression was detectable in colon and lung (23). However, *HTR3D* could not be amplified from kidney, and weak bands were visible in brain tissue from caudate nucleus and hippocampus and in the periphery in liver, heart, and stomach. Primers for *HTR3E* were also suitable to amplify *HTR3Ea*. Consistent with earlier studies, expression of *HTR3E* was restricted to colon and intestine (23, 34). The mRNA for canonical *RIC3* (RIC-3a; band size, 1.18 kb) was expressed in all tissues tested except kidney. Thus, it was present in those tissues expressing at least one of the 5-HT3 subunits A, C, D, or E. Three additional products with sizes of approximately 1.0, 0.8, and 0.6 kb could be amplified, presenting with a tissue-specific expression pattern. These might presumably correspond to splice isoforms of *RIC3*, which have been described previously (12, 35).
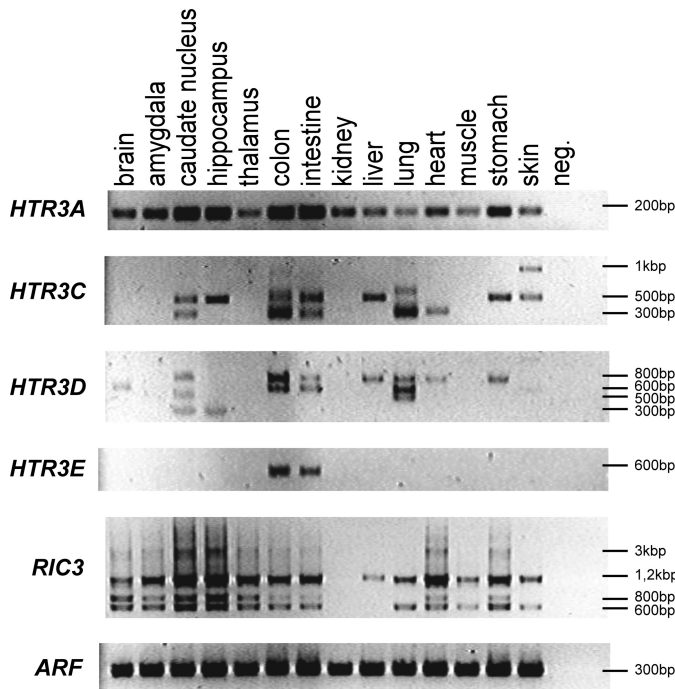
FIGURE 1. **Comparative mRNA expression analysis.** Reverse transcription-PCR analysis of the genes *HTR3A*, *-C*, *-D*, *-E*, and *RIC3* using cDNAs from 14 different human adult tissues. Expression of ADP-ribosylation factor (*ARF*) was used as a control for cDNA integrity. *neg.*, negative control.
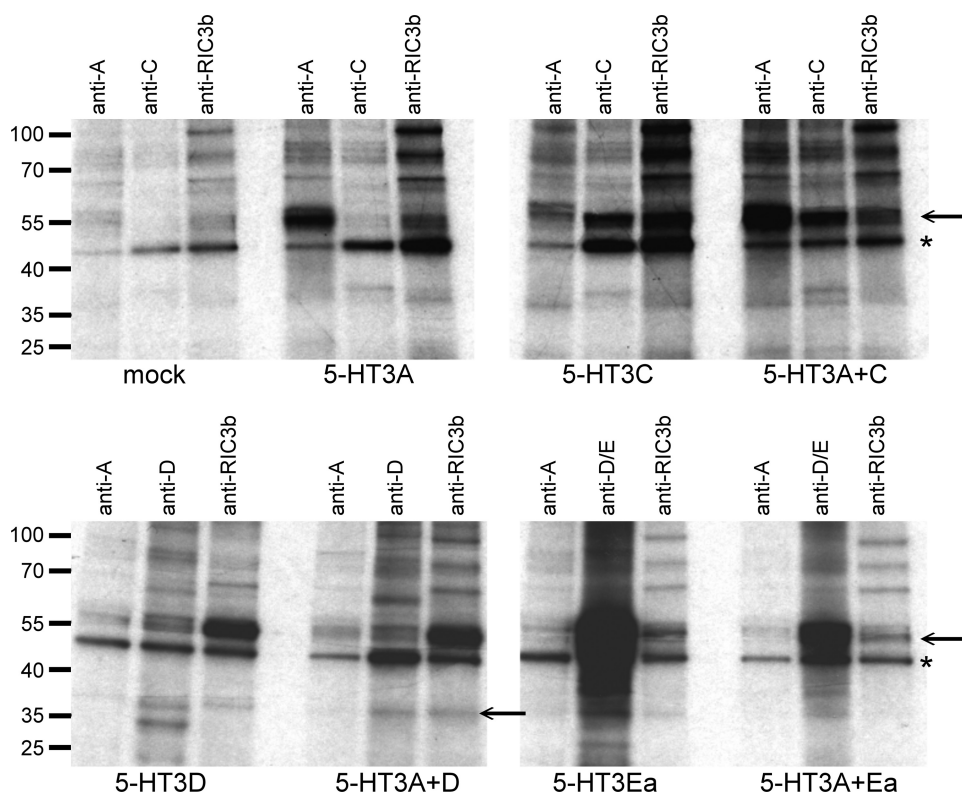
Co-localization of 5-HT3C, -D, or -Ea and Calnexin or RIC-3

Immunofluorescence experiments of two different mammalian cell lines (HEK293 and U2OS) transiently expressing 5-HT3C, -D, or -Ea subunits revealed a co-staining of these subunits with the ER-resident chaperone calnexin and thereby confirmed the localization of the 5-HT3 subunits to the ER (supplemental Fig. 1). To obtain insight into the possible interaction of the 5-HT3 subunits and the more specific chaperone RIC-3, further immunofluorescence experiments on the same cell lines transiently expressing 5-HT3C, -D, or -Ea subunits and RIC-3 were carried out.

FIGURE 2. **Co-localization of 5-HT3 subunits and RIC-3 in ER.** Immunofluorescence analysis of transfected HEK293 and U2OS cells expressing Myc-/HA-tagged 5-HT3C, -D, or -Ea subunit. The negative control is pcDNA3 empty vector (mock-transfected cells). Antibodies used were either mouse anti-HA (Sigma) or mouse anti-Myc (Cell Signaling Technology, 9E10), and sheep anti-RIC-3. Secondary antibodies were either anti-mouse Alexa Fluor 488 or anti-sheep Alexa Fluor 546 (Invitrogen). The 5-HT3 subunits are stained in *green*; RIC-3 is visualized in *red*. Cells were 4′,6-diamidino-2-phenylindole-counterstained to visualize nuclei in *blue*.

FIGURE 3. **Interaction of 5-HT3 subunits with RIC-3.** Protein lysates of HEK293 cells transiently expressing different 5-HT3 subunit combinations (denoted *below* the pictures) and RIC-3 were used for immunoprecipitation with 5-HT3 subunit-specific antibodies or an anti-RIC-3 antibody (denoted *above* the pictures) after [^{35}S]methionine/cysteine labeling followed by SDS-polyacrylamide gel electrophoresis and autoradiography. The *asterisk* denotes a nonspecific band present in all approaches. *Arrows* point at 5-HT3 subunit-specific immunoreactive bands.

These experiments revealed a co-localization of all tested subunits and RIC-3 in the ER (Fig. 2).

Direct Interaction of 5-HT3C, -D, and -Ea with BiP/Calnexin

To further analyze the putative interaction between the subunits 5-HT3A, -C, -D, and -E and the globally acting ER-resident chaperones BiP and calnexin, immunoprecipitation experiments of transfected and metabolically labeled HEK293 cells were performed. A direct protein interaction between 5-HT3A, -C, and -Ea and the two chaperones was confirmed because all subunits co-precipitated with BiP or calnexin. In the case of 5-HT3D, a direct BiP or calnexin interaction remained questionable in this experimental setup because the expected band was hardly visible (supplemental Fig. 2A). However, additional immunoprecipitation experiments followed by Western blot confirmed an interaction of 5-HT3D with BiP or calnexin (supplemental Fig. 2B).

Direct Interaction of 5-HT3A, -C, -D, and -Ea with RIC-3 and N-Glycosylation of 5-HT3C and -Ea

To additionally determine the existence of direct protein interactions between the subunits 5-HT3A, -C, -D, and -E and RIC-3, the same technique as that used for calnexin and BiP was applied. For that purpose, specific antibodies raised against the 5-HT3 subunits A, C, D, and E and RIC-3 were used

(supplemental Table 2) (16).[3] The interaction of RIC-3 with the 5-HT3B subunit could not be studied because no suitable antibody was available. Previous experiments revealed that the 5-HT3D/E antibody works better for the isoform 5-HT3Ea than for 5-HT3E. Thus, our analysis was restricted to only 5-HT3Ea. Immunoreactive bands of expected sizes were detectable for 5-HT3A, -C, and -Ea (approximately 55 kDa) and for 5-HT3D (approximately 35 kDa) (Fig. 3). In lysates of cells co-transfected with RIC-3 and 5-HT3 subunit cDNAs, the corresponding immunoreactive bands for the 5-HT3 subunits were detected by anti-RIC-3, indicating that RIC-3 co-precipitated with 5-HT3A, -C, -D, and -Ea subunits.

The co-immunoprecipitation of RIC-3 and 5-HT3A revealed an immunoreactive band of a size below that of the completely glycosylated 5-HT3A subunit. This finding indicates that RIC-3 might exclusively interact with only partially glycosylated and thus immature 5-HT3A subunits. In contrast, RIC-3 co-precipitated with 5-HT3C, -D, and -Ea bands of all sizes, representing differentially glycosylated subunits in the case of 5-HT3C and -Ea that would fit to the expected size increase of approximately 3 kDa per *N*-glycosylation site (37). In Western blot experiments on transfected cells pretreated with tunicamycin, block of *N*-linked glycosylation led to a loss of higher molecular mass bands for 5-HT3C and -Ea. In contrast, the band for 5-HT3D remained unchanged (Fig. 4*A*). This suggests that *N*-glycosylation does occur on 5-HT3C and -Ea, whereas 5-HT3D is not glycosylated as has been predicted previously (23). All predicted *N*-glycosylation sites were verified by Western blot analysis of cells expressing 5-HT3C or -Ea after knock-out of the respective sites (23) using site-directed mutagenesis (Fig. 4*B*).

Influence of RIC-3 on 5-HT-induced Ca²⁺ Influx through 5-HT₃ Receptors

Homomeric 5-HT₃A Receptors—5-HT led to concentration-dependent aequorin luminescence reflecting intracellular Ca²⁺ elevation when applied to coelenterazine *h*-loaded HEK293 cells transiently expressing apoaequorin, RIC-3, and 5-HT3A. The resulting concentration-response curve was characterized by a pEC₅₀ value of 5.77 ± 0.02 and a Hill coefficient of 3.12 ± 0.22. These functional parameters did not differ from those

---

[3] J. Kapeller, D. Moeller, M.-T. Liu, F. Lasitschka, F. Autschbach, R. Hovius, G. Rappold, M. Brüss, M. D. Gershon, and B. Niesler, manuscript in preparation.
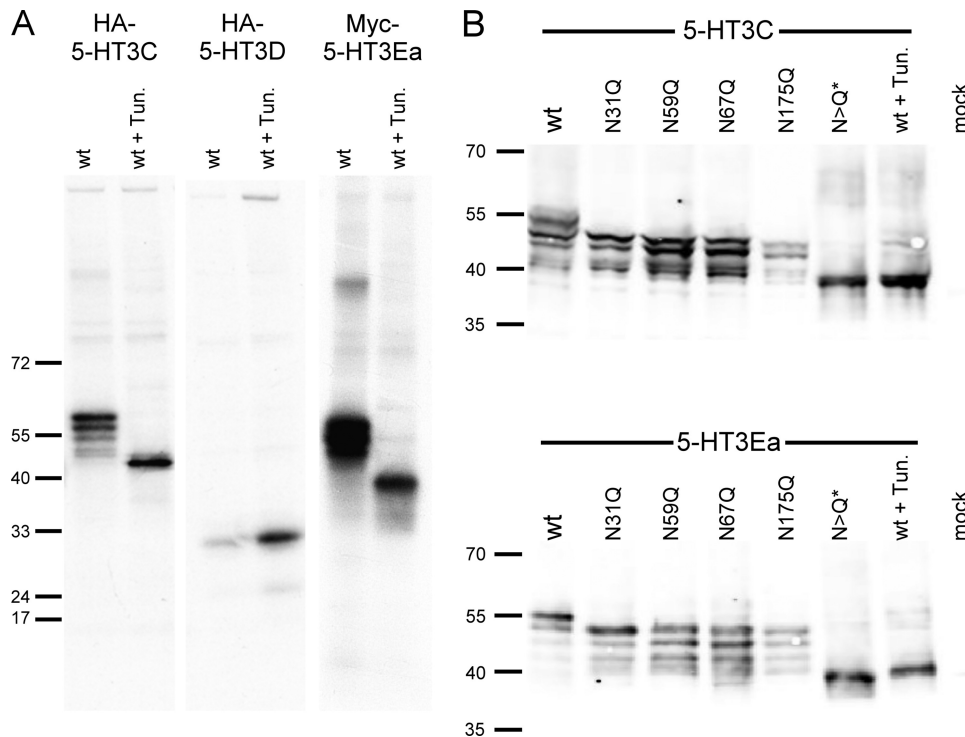
FIGURE 4. **Glycosylation studies of 5-HT3C, -D and -Ea.** *A*, immunoprecipitation of metabolically labeled proteins of HEK293 cells expressing Myc-/HA-tagged 5-HT3C, -D, and -Ea subunits. Immunoprecipitation was carried out with an anti-HA or an anti-Myc antibody, respectively. Proteins were separated on a 4–12% Bis-Tris NuPAGE gel (Invitrogen) followed by autoradiography. To check for glycosylation of the respective subunit, one batch was treated with tunicamycin, and the other was not. Immunoreactive bands of approximately 50–60 kDa (HA-5-HT3C), approximately 30 kDa (HA-5-HT3D), and approximately 60 kDa (Myc-5-HT3Ea) were detectable for untreated cells. After tunicamycin treatment, no effect was detectable for 5-HT3D, whereas the band sizes for 5-HT3C and 5-HT3Ea were reduced to approximately 40 kDa, respectively. *B*, Western blot of *N*-glycosylation knock-out constructs generated by site-directed mutagenesis, affecting either one of four predicted *N*-glycosylation sites (N31Q, N59Q, N67Q, or N175Q) in 5-HT3C and 5-HT3Ea or all of them (*N>Q**). HEK293 cells were transfected with 5-HT3C or -Ea constructs, and one batch of the wild-type (*wt*) subunits was treated with tunicamycin (*Tun.*). Proteins were separated on a 4–12% Bis-Tris NuPAGE gel (Invitrogen) and blotted on polyvinylidene difluoride membranes. Subunit-specific antibodies were used for detection following the Odyssey Western Blot Analysis protocol (Li-Cor Biosciences). Immunoreactive bands of approximately 40–55 kDa were detectable with the upmost band (55 kDa) missing in the case of the single knock-outs. The N>Q* knockouts and the tunicamycin-treated cells showed only one band at approximately 40 kDa.

5-HT3A + 5-HT3E did not significantly differ from that determined on cells expressing the homomeric 5-HT₃A receptor (274.1 ± 30.2 and 262.4 ± 27.4%, respectively). In contrast, RIC-3 led to a significantly smaller increase of E_{max} on 5-HT₃AB receptors of 179.0 ± 14.6% compared with that on 5-HT₃A receptors. The most prominent influence of RIC-3 was detected on cells expressing 5-HT3A + 5-HT3C or 5-HT3A + 5-HT3Ea. The E_{max} values were increased to 426.5 ± 32.1 and 513.4 ± 37.0%, respectively, in the presence of RIC-3 (Fig. 6).

### Influence of RIC-3 on Cell Surface Expression of 5-HT₃ Receptors of Diverse Composition

[³H]GR6530 Binding Studies— The enhancement of human 5-HT₃A receptor cell surface expression by human RIC-3 in mammalian cells has been shown before (16). Thus, we hypothesized that the increased 5-HT E_{max} values for Ca²⁺ influx reflect the promotion of cell surface expression by RIC-3. To clarify this issue, saturation binding studies with the 5-HT₃ antagonist [³H]GR65630 on membranes from transfected HEK293 cells were carried out. Experiments were performed for homomeric 5-HT₃A receptors and specific 5-HT3 subunit combinations, which

determined on 5-HT₃A receptors in the absence of RIC-3 (pEC₅₀, 5.76 ± 0.03; Hill coefficient, 3.19 ± 0.26) (Fig. 5*A*). By contrast, RIC-3 increased the 5-HT-induced E_{max}. The RIC-3-mediated elevation of E_{max} depended on the RIC-3 cDNA amount (Fig. 5*B*). Significantly increased Ca²⁺ responses were detected for 5-HT3A:RIC-3 cDNA ratios between 1:0.01 and 1:1. The maximum RIC-3 effect was observed with a 1:0.1 cDNA ratio (279.9 ± 16.9% of control in the absence of RIC-3). For this reason, the 5-HT3 subunit:RIC-3 cDNA ratio 1:0.1 was used for further experiments.

Co-expression of 5-HT3A and 5-HT3B (or -C, -D, -E, or -Ea)— To determine the impact of RIC-3 on different 5-HT3 subunit combinations, cells expressing 5-HT3A (homomeric 5-HT₃A receptor as control) or 5-HT3A + 5-HT3B (or -C, -D, -E, or -Ea) in the presence or absence of RIC-3 were analyzed for 5-HT-induced maximum Ca²⁺ responses. In analogy to the results described above, 5-HT induced a significantly higher maximum response of 298.5 ± 21.9% in cells expressing 5-HT3A and RIC-3 compared with the response in the absence of RIC-3 (Student's *t* test, *p* < 0.001). The RIC-3-mediated increases of E_{max} on cells expressing 5-HT3A + 5-HT3D or

exhibited a significantly different influence of RIC-3 on the 5-HT-induced E_{max} compared with the effect of RIC-3 on the 5-HT₃A receptor, *i.e.* 5-HT3A + 5-HT3B (or -C or -Ea) (see above). Co-expression of RIC-3 and 5-HT3A led to an increase of the B_{max} of [³H]GR65630 to 232.7 ± 21.0% compared with the B_{max} in the absence of RIC-3 (Student's *t* test, *p* < 0.001). This is related to an increase of the cell surface expression of the receptor (Table 2). RIC-3 also led to enhanced B_{max} values for the examined 5-HT3 subunit combinations, however, to different extents as compared with increases in 5-HT-induced E_{max} (Table 2). Co-expression of RIC-3 together with 5-HT3A + 5-HT3C and 5-HT3A + 5-HT3Ea resulted in B_{max} increases of 319.0 ± 17.9 and 317.5 ± 22.2%, respectively. These values are significantly higher than the RIC-3-mediated B_{max} increase of the homomeric 5-HT₃A receptor. On the other hand, the B_{max} determined on cells transfected with 5-HT3A + 5-HT3B cDNAs was less elevated in the presence of RIC-3 (184.1 ± 12.6%) than that of homomeric 5-HT₃A receptors; however, the significance level was not reached in this case (Fig. 6 and Table 2). As expected, the dissociation constants (K_d) for [³H]GR65630 on the examined receptors were not different in the presence or absence of RIC-3 (Table 2).

A

B
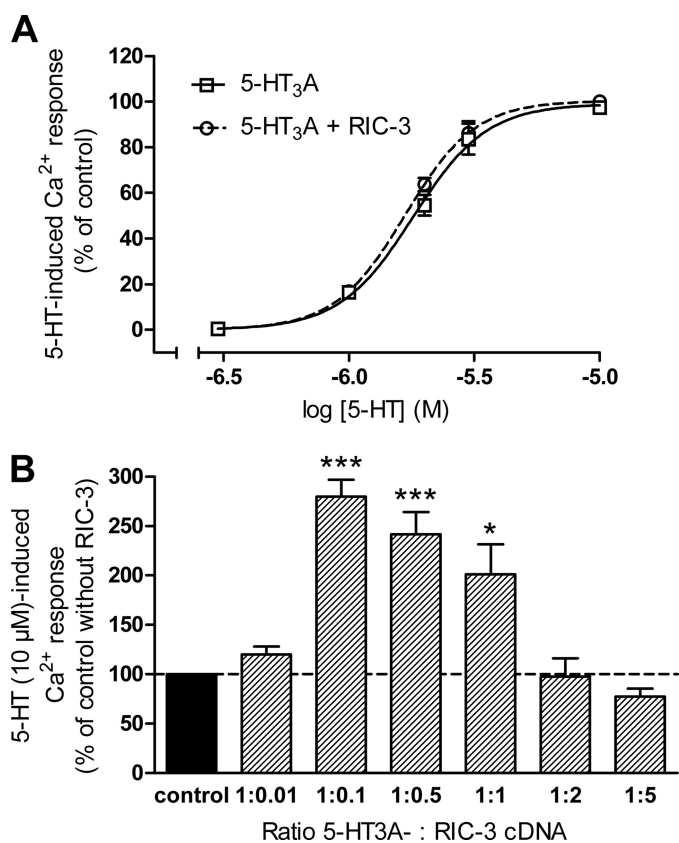
FIGURE 5. Influence of RIC-3 on 5-HT-induced Ca^{2+} influx through homomeric 5-HT$_3$A receptors transiently expressed in HEK293 cells. *A*, concentration-response curves for 5-HT-induced Ca^{2+} influx on coelenterazine *h*-loaded cells expressing apoaequorin and 5-HT3A in the presence or absence of RIC-3. Shown are means ± S.E. of 4–11 independent transfections expressed as percentage of the respective 5-HT-maximum response. Equal amounts of 5-HT3A and RIC-3 cDNAs were used. *B*, 5-HT (10 μM)-induced maximum responses in relation to the RIC-3 cDNA amounts used for transfection. *Bars* represent mean values ± S.E. of 3–14 independent experiments expressed as percentage of the response in the absence of RIC-3 (control). The same 5-HT3A cDNA amount was used for all transfections. Significant differences compared with control in the absence of RIC-3 are indicated: *, $p < 0.05$; ***, $p < 0.001$.
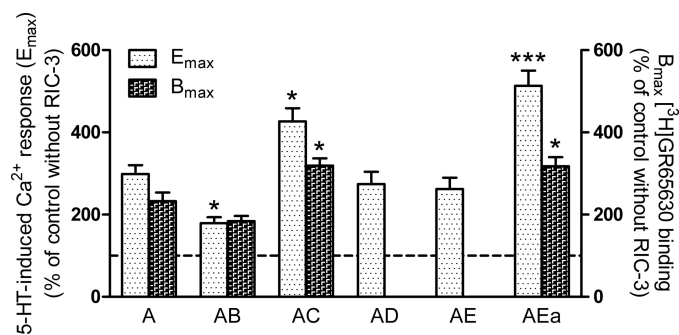
FIGURE 6. Effect of RIC-3 on 5-HT-induced maximum Ca^{2+} influx and on B_{max} values for [^{3}H]GR65630 binding of HEK293 cells transiently expressing either 5-HT3A or 5-HT3A + 5-HT3B (or -C, -D, -E, or -Ea). B_{max} values for [^{3}H]GR65630 were calculated from six independent saturation binding experiments on membrane fragments. Maximum 5-HT-induced Ca^{2+} responses (E_{max}), measured as aequorin luminescence, were recorded in 8–10 independent experiments using a 5-HT concentration of 10 μM (or 500 μM for 5-HT3A + 5-HT3B). Values (means ± S.E.) are expressed as percentage of the respective control in the absence of RIC-3. Significant differences compared with the RIC-3-mediated effects on the homomeric 5-HT$_3$A receptor are indicated: *, $p < 0.05$; ***, $p < 0.001$.

Flow Cytometry Experiments—Because the radioligand [^{3}H]GR65630 does not allow discrimination between heteromeric and homomeric 5-HT$_3$ receptors, an immunocytochemical approach was additionally applied. Therefore, FACS analyses with Myc-/HA-tagged subunits to enable the cell surface detection of particular subunits in cells expressing 5-HT3A + 5-HT3B (or -C, -D, -E, or -Ea) were carried out. In one set of experiments, cells expressing the HA-tagged 5-HT3A subunit plus one of the Myc-tagged 5-HT3B, -E, and -Ea subunits or the empty plasmid vector (HA-5-HT3A as control) in the presence or absence of RIC-3 were measured. In another set, cells expressing the Myc-tagged 5-HT3A subunit plus one of the HA-tagged 5-HT3C and -D subunits or the empty plasmid vector (Myc-5-HT3A as control) were analyzed.

Detection of HA-5-HT3A and Myc-5-HT3A in cells exclusively expressing 5-HT3A subunits revealed significantly enhanced FIs, reflecting increases of surface expression of homomeric 5-HT$_3$A receptors to 181.2 ± 17.2 and 161.0 ± 10.43% of control, respectively, in the presence of RIC-3 (Fig. 7). RIC-3 also mediated significant elevation of cell surface expression of 5-HT3A subunits when co-expressed with 5-HT3E or 5-HT3D subunits to 201.7 ± 10.13 and 146.6 ± 8.4% of control, respectively. These increases were not significantly different from those measured for the corresponding homomeric 5-HT$_3$A receptor. In contrast, co-expression of 5-HT3Ea or 5-HT3C subunits led to significantly higher RIC-3-mediated increases of the cell surface expression of 5-HT3A subunits compared with that for the 5-HT$_3$A receptor expressed alone (252.3 ± 22.72 and 195.0 ± 11.04%, respectively). Unexpectedly, the 5-HT3C, -D, -E, and -Ea subunits seemed to be expressed at very low frequencies on the surface of HEK293 cells. An average number of about 3% positive cells could be measured for these subunits, whereas for 5-HT3A the number of positive cells ranged from about 19 to 40% in the absence of RIC-3 (data not shown). Co-expression of RIC-3 did not alter the expression of 5-HT3C, -D, -E, and -Ea subunits on the cell surface (data not shown). In contrast, Myc-5-HT3B was well detectable on the cell surface, and RIC-3 led to an increased surface expression of HA-5-HT3A after co-expression of Myc-5-HT3B to 150.9 ± 15.0% of control. However, the expression of Myc-5-HT3B itself was not altered by RIC-3 (110.8 ± 14.7% of control).

DISCUSSION

Only a limited amount of information exists on the regulation of 5-HT$_3$ receptor expression and composition in different tissues. Therefore, we investigated the impact of the chaperone RIC-3 on the surface expression and function of diverse 5-HT$_3$ receptors, focusing on the 5-HT3C, -D, and -E subunits. Comparative mRNA expression analysis showed expression of alternative *RIC3* transcripts in human tissues expressing at least one of the subunits 5-HT3C, -D, and -E. This is in line with the ubiquitous expression of *RIC3* mRNA in central and peripheral tissues that has been shown in previous studies (12, 35). Thus, RIC-3 is likely to be co-expressed in cells expressing 5-HT$_3$ receptors, enabling interactions between the chaperone and 5-HT3 subunits *in vivo*. Furthermore, we showed co-localization of RIC-3 and 5-HT3C, -D, and -E subunits in the ER of two

mammalian cell lines. Direct interaction of RIC-3 and the 5-HT3A subunit has been shown previously by co-immunoprecipitation (16). Our co-immunoprecipitation studies with HEK293 cells expressing 5-HT3 subunits and RIC-3 revealed that RIC-3 does not only interact with 5-HT3A but also with 5-HT3C, -D, and -Ea. Because the splice isoform 5-HT3Ea only differs from 5-HT3E in its signal sequence at the very N-terminal end (28), RIC-3 interaction with 5-HT3E is very likely. However, comparative expression analysis suggests that the RIC-3-mediated regulation of 5-HT$_3$ receptor expression might be even more complex because, in the case of *HTR3C* and *HTR3D*, splice variants were detectable. The existence of additional *HTR3* splice variants was described recently (33). Consequently, their role in receptor assembly and trafficking requires further investigation.

Analogous co-immunoprecipitation experiments with BiP and calnexin also revealed a direct interaction of these generalized chaperones with 5-HT3A, -C, -D, and -Ea subunits that previously has only been shown for 5-HT$_3$AB receptors (6). Interaction with these chaperones *in vivo* is very likely because they are co-localized with 5-HT3 subunits in the ER, which was shown for calnexin by immunofluorescence. Additional findings regarding posttranslational modification of the subunits 5-HT3C, -D, -E, and -Ea came from *N*-glycosylation studies of transfected HEK293 cells. So far, *N*-glycosylation has only been shown for the subunits 5-HT3A and -B (6, 37). Our experiments revealed that all tested subunits except 5-HT3D are *N*-glycosylated and confirmed the previously predicted glycosylation sites (23). This points to an additional layer of complexity in the 5-HT$_3$ receptor system based on posttranslational modification, which might play a role in receptor maturation and surface expression as has been shown for γ-aminobutyric acid type A and 5-HT$_3$A receptors (37, 38). Interestingly, interaction of RIC-3 with the 5-HT3A subunit was shown to be restricted to only partially glycosylated subunits, which would be consistent with its role in retaining immature but releasing mature 5-HT3A from the ER. In contrast, RIC-3 interacted with 5-HT3C and -Ea of all glycosylated states, suggesting that both immature and mature subunits are retained in the ER by RIC-3. This suggests a differential regulation of the expression of 5-HT3A compared with other 5-HT3 subunits by RIC-3 (see below).
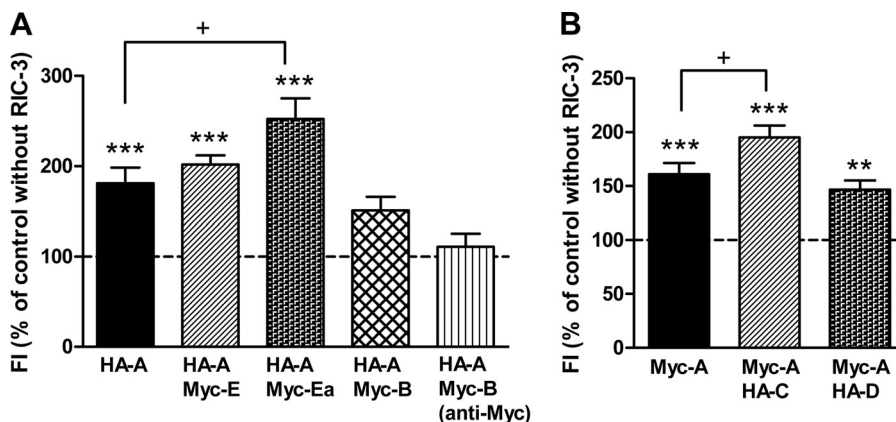
Recent studies revealed a RIC-3-mediated increase of cell surface expression of functional nACh and 5-HT$_3$A receptors. The ability of RIC-3 to act as a chaperone seems to be influenced by the host cell environment. Consistent with this, human RIC-3 enhanced the cell surface expression of recombinant human 5-HT$_3$A receptors in mammalian cells (9, 13, 16), whereas it led to inhibition of recombinant murine 5-HT$_3$A receptors in *Xenopus* oocytes (12, 39). In consideration of these species- and cell-dependent effects, we studied the impact of human RIC-3 on human 5-HT3 subunits heterologously expressed in HEK293 cells. As previously reported, RIC-3 exhibited no influence on the potency of the agonist 5-HT on homomeric 5-HT$_3$A receptors (16). Furthermore, the affinities of the radioligand [^{3}H]GR65630 to all tested 5-HT3 subunit combinations were not altered after RIC-3 co-expression. Thus, RIC-3 does not influence the conformation of the 5-HT$_3$ receptor ligand-binding site. These results suggest that RIC-3 does not affect the function of 5-HT$_3$ receptors. As expected from its action as a chaperone, radioligand binding and functional Ca^{2+} influx studies revealed that RIC-3 enhances the cell surface expression of functional 5-HT$_3$ receptors in particular for all tested 5-HT3 subunit combinations, *i.e.* 5-HT3A and 5-HT3A + 5-HT3B (or -C, -D, -E, or -Ea).

As determined by measuring maximum 5-HT-induced Ca^{2+} influx through homomeric 5-HT$_3$A receptors, the RIC-3-mediated increase of receptor expression was strongly dependent on the RIC-3 levels. RIC-3 enhanced maximum Ca^{2+} responses in cells with 5-HT3A:RIC-3 cDNA ratios of 1:0.01

TABLE 2

Binding parameters from [³H]GR65630 saturation binding on membrane fragments of HEK293 cells transiently expressing either 5-HT3A or 5-HT3A + 5-HT3B (or -C or -Ea) in presence or absence of RIC-3

Saturation binding was performed by incubation of membranes with five increasing concentrations of the 5-HT$_3$ antagonist [³H]GR65630 (0.02–1.5 nM). Non-specific binding was determined on membranes of mock-transfected cells. Values shown are mean ± S.E. of six independent experiments. Significant differences compared with the respective control in the absence of RIC-3 (Student's *t* test) are indicated.

Subunits	B_{max}		K_d	
	−RIC-3	+RIC-3	−RIC-3	+RIC-3
	pmol/mg protein		*nM*	
5-HT3A	25.01 ± 2.26	57.80 ± 4.55[a]	0.09 ± 0.01	0.10 ± 0.01
5-HT3A + 5-HT3B	5.01 ± 0.35	9.22 ± 0.90[b]	0.08 ± 0.01	0.08 ± 0.01
5-HT3A + 5-HT3C	7.89 ± 1.28	24.47 ± 3.43[b]	0.06 ± 0.01	0.07 ± 0.01
5-HT3A + 5-HT3Ea	4.11 ± 0.42	12.73 ± 1.01[a]	0.05 ± 0.01	0.07 ± 0.01

[a] $p < 0.001$.
[b] $p < 0.01$.

FIGURE 7. **Flow cytometry analysis of HEK293 cells transiently expressing either 5-HT3A or 5-HT3A + 5-HT3B (or -C, -D, -E, or -Ea) in the presence or absence of RIC-3.** Cells were transfected with Myc- or HA-tagged subunit cDNAs to enable the cell surface detection with mouse anti-HA (clone HA-7) or mouse anti-Myc antibody (clone 9B11). The secondary antibody was Alexa Fluor 488 donkey anti-mouse IgG. FIs are expressed as percentages of the respective FI values in the absence of RIC-3 (means ± S.E. of six to nine independent transfections). Shown is the cell surface expression of the 5-HT3A subunit detected by anti-HA (*A*) or anti-Myc antibody (*B*). For co-transfections of 5-HT3A and 5-HT3B cDNA, expression of both subunits is shown (*A*). Significant differences compared with control without RIC-3 (**, $p < 0.01$; ***, $p < 0.001$) or compared with the RIC-3 effect on the homomeric 5-HT$_3$A receptor (+, $p < 0.05$) are indicated.

to 1:1. Further increase of the RIC-3 cDNA amount abolished the RIC-3-mediated elevation of the maximum Ca^{2+} signal. This might be due to the formation of RIC-3 aggregates, which have been observed after RIC-3 overexpression (17, 40, 41) and shown to reduce the amount of nACh receptor subunits for the formation of functional receptors (40). This is in line with a recent study showing that co-expression of RIC-3 and the nAChα7 subunit in tsA201 cells only led to a measurable cell surface expression of the homomeric nAChα7 receptor when small amounts of RIC-3 cDNA were used (42). This concentration dependence of the chaperone activity of RIC-3 might be an essential mechanism of the expression regulation of nACh and 5-HT$_3$ receptors in different cell types or at different times. Cheng *et al.* (16) also observed an enhanced surface expression of 5-HT3A subunits depending on the RIC-3 amount. However, they found an increase of surface expression of 5-HT3A up to a 5-HT3A:RIC-3 cDNA ratio of 1:4. These discrepancies might be due to application of different expression constructs or to different incubation times after transfection because the interaction with RIC-3 was shown to be transient (16).

The extent of the RIC-3-mediated increase of cell surface expression varied between different 5-HT3 subunit combinations. This was shown by three approaches: 5-HT-induced Ca^{2+} influx, radioligand saturation binding, and FACS studies. FACS analyses revealed that on cells co-expressing 5-HT3A and 5-HT3B subunits RIC-3 exclusively enhanced cell surface expression of 5-HT3A, whereas the amount of 5-HT3B remained constant. Hence, a predominant formation of homomeric 5-HT$_3$A receptors at the expense of heteromeric 5-HT$_3$AB receptors is promoted. This result confirms data of recent studies (17, 30). The net effect was therefore a less pronounced RIC-3-mediated increase in 5-HT$_3$ receptor surface expression on cells expressing 5-HT3A + 5-HT3B compared with cells exclusively expressing 5-HT3A. This was seen in both Ca^{2+} influx and radioligand binding studies and is further supported by data of Cheng *et al.* (17), who also measured a slightly smaller RIC-3-induced increase of B_{max} for [^{3}H]GR65630 binding on cells expressing 5-HT3A + 5-HT3B compared with those exclusively expressing 5-HT3A.

Unexpectedly, FACS experiments on cells co-expressing 5-HT3A and 5-HT3C (or -D, -E, or -Ea) subunits revealed that 5-HT3C, -D, -E, and -Ea are expressed on the cell surface at very low levels, which were not increased by RIC-3. The lack of an RIC-3-mediated increase of surface expression of 5-HT3C, -D, -E, and -Ea would be in line with its interaction with mature subunits. Thus, comparable with its reported action on the 5-HT3B subunit, RIC-3 appears to have an inhibitory effect on these subunits as well. Their marginal surface expression levels, measured in FACS experiments, seem to contradict results from previous immunofluorescence and biotinylation studies showing co-expression of 5-HT3A and 5-HT3C (or -D, -E, or -Ea) on the cell surface (28). However, immunofluorescence images showed a lower fluorescence intensity for the subunits 5-HT3C, -D, -E, and -Ea compared with 5-HT3A on the cell surface (see Fig. 1 in Ref. 28). Low levels of surface expression restricted to a small number of cells, visible in immunofluorescence, are likely to be missed in flow cytometry, which is less sensitive. We conclude that only a low amount of the subunits

5-HT3C, -D, -E, and -Ea is part of mature receptors on the cell surface of HEK293 cells. This might be one reason why no differences in the pharmacological properties of cells expressing 5-HT3A + 5-HT3C (or -D, -E, or -Ea) and those expressing homomeric 5-HT$_3$A receptors could be detected until now (28). Furthermore, an explanation for the lacking surface expression of these subunits could be the requirement of yet unidentified chaperones for incorporation into functional 5-HT$_3$ receptors, which are not present in HEK293 cells. This would be comparable with the situation regarding nAChα7 receptors some years ago. Efficient surface expression of these receptors in cell lines like HEK293 or Chinese hamster ovary was not achieved until the discovery of RIC-3 as an nACh receptor chaperone (15, 43).

RIC-3 mediated the most prominent increase of 5-HT$_3$ receptor cell surface expression on cells expressing 5-HT3A + 5-HT3Ea (or -C) measured by radioligand binding and 5-HT-induced Ca^{2+} influx. This was confirmed by FACS analyses showing that the RIC-3-mediated increase of surface expression of the 5-HT3A subunit was highest on these cells. Cells expressing the latter subunit combinations have been shown previously to exhibit significantly lower 5-HT$_3$ receptor surface expression levels compared with cells expressing homomeric 5-HT$_3$A receptors (28, 30, 33). Thus, we hypothesize that the inhibitory effect of 5-HT3Ea and -C subunits on 5-HT$_3$ receptor expression might be abolished by RIC-3, leading to a facilitated cell surface expression of mature homomeric 5-HT$_3$A receptors. On the other hand, the RIC-3-mediated increases of 5-HT$_3$ receptor cell surface expression on cells expressing 5-HT3A + 5-HT3D (or -E) were not different from that on cells expressing homomeric 5-HT$_3$A receptors. This is in agreement with the fact that these subunit combinations did not alter 5-HT$_3$ receptor surface expression compared with cells expressing homomeric 5-HT$_3$A receptors (28). However, the question whether this kind of regulation would be the same in native cells, which express the required chaperones, still remains. Thus, the function of the subunits 5-HT3C, -D, and -E is still elusive, and the discovery of yet unidentified essential chaperone molecules will enable further studies regarding 5-HT$_3$ receptor composition.

In summary, we showed interaction of the two general chaperones BiP and calnexin and the specific chaperone RIC-3 with 5-HT3A, -C, -D, and -E subunits. Combined with previous findings (17), our results support the hypothesis that RIC-3 serves to ensure the production of homomeric 5-HT$_3$A receptors at the expense of heteromeric receptors incorporating 5-HT3B–E subunits. Therefore, RIC-3 seems to play an important role in determining 5-HT$_3$ receptor composition *in vivo*. Analogous results have been reported for nACh receptors of *C. elegans*; RIC-3 led to a preferential expression of DEG-3-rich DEG-3/DES-2 receptors (26, 27). Interestingly, *RIC3* mRNA levels have been shown to be elevated in the post-mortem brains of individuals with bipolar disorder and schizophrenia (18), and accumulating evidence exists that 5-HT$_3$ receptors are likely to be involved in both diseases (36).[3] This underlines the putative role of 5-HT$_3$ receptor modulation by RIC-3, which might be disturbed in neuropsychiatric diseases. Therefore, the investigation of 5-HT$_3$ receptor maturation and regulation will

help to gain insight into the pathomechanism and to generate novel approaches for the therapy of these diseases.

REFERENCES

1. Collingridge, G. L., Isaac, J. T., and Wang, Y. T. (2004) *Nat. Rev. Neurosci.* **5,** 952–962
2. Green, W. N., and Millar, N. S. (1995) *Trends Neurosci.* **18,** 280–287
3. Blount, P., and Merlie, J. P. (1991) *J. Cell Biol.* **113,** 1125–1132
4. Gelman, M. S., Chang, W., Thomas, D. Y., Bergeron, J. J., and Prives, J. M. (1995) *J. Biol. Chem.* **270,** 15085–15092
5. Wanamaker, C. P., and Green, W. N. (2007) *J. Biol. Chem.* **282,** 31113–31123
6. Boyd, G. W., Low, P., Dunlop, J. I., Robertson, L. A., Vardy, A., Lambert, J. J., Peters, J. A., and Connolly, C. N. (2002) *Mol. Cell. Neurosci.* **21,** 38–50
7. Vandenberghe, W., Nicoll, R. A., and Bredt, D. S. (2005) *J. Neurosci.* **25,** 1095–1102
8. Jeanclos, E. M., Lin, L., Treuil, M. W., Rao, J., DeCoster, M. A., and Anand, R. (2001) *J. Biol. Chem.* **276,** 28281–28290
9. Millar, N. S. (2008) *Br. J. Pharmacol.* **153,** Suppl. 1, S177–S183
10. Nguyen, M., Alfonso, A., Johnson, C. D., and Rand, J. B. (1995) *Genetics* **140,** 527–535
11. Halevi, S., McKay, J., Palfreyman, M., Yassin, L., Eshel, M., Jorgensen, E., and Treinin, M. (2002) *EMBO J.* **21,** 1012–1020
12. Halevi, S., Yassin, L., Eshel, M., Sala, F., Sala, S., Criado, M., and Treinin, M. (2003) *J. Biol. Chem.* **278,** 34411–34417
13. Lansdell, S. J., Collins, T., Yabe, A., Gee, V. J., Gibb, A. J., and Millar, N. S. (2008) *J. Neurochem.* **105,** 1573–1581
14. Lansdell, S. J., Gee, V. J., Harkness, P. C., Doward, A. I., Baker, E. R., Gibb, A. J., and Millar, N. S. (2005) *Mol. Pharmacol.* **68,** 1431–1438
15. Williams, M. E., Burton, B., Urrutia, A., Shcherbatko, A., Chavez-Noriega, L. E., Cohen, C. J., and Aiyar, J. (2005) *J. Biol. Chem.* **280,** 1257–1263
16. Cheng, A., McDonald, N. A., and Connolly, C. N. (2005) *J. Biol. Chem.* **280,** 22502–22507
17. Cheng, A., Bollan, K. A., Greenwood, S. M., Irving, A. J., and Connolly, C. N. (2007) *J. Biol. Chem.* **282,** 26158–26166
18. Severance, E. G., and Yolken, R. H. (2007) *Neuroscience* **148,** 454–460
19. Belelli, D., Balcarek, J. M., Hope, A. G., Peters, J. A., Lambert, J. J., and Blackburn, T. P. (1995) *Mol. Pharmacol.* **48,** 1054–1062
20. Davies, P. A., Pistis, M., Hanna, M. C., Peters, J. A., Lambert, J. J., Hales, T. G., and Kirkness, E. F. (1999) *Nature* **397,** 359–363
21. Dubin, A. E., Huvar, R., D'Andrea, M. R., Pyati, J., Zhu, J. Y., Joy, K. C., Wilson, S. J., Galindo, J. E., Glass, C. A., Luo, L., Jackson, M. R., Lovenberg,
22. T. W., and Erlander, M. G. (1999) *J. Biol. Chem.* **274,** 30799–30810
22. Miyake, A., Mochizuki, S., Takemoto, Y., and Akuzawa, S. (1995) *Mol. Pharmacol.* **48,** 407–416
23. Niesler, B., Frank, B., Kapeller, J., and Rappold, G. A. (2003) *Gene* **310,** 101–111
24. Chetty, N., Coupar, I. M., Tan, Y. Y., Desmond, P. V., and Irving, H. R. (2009) *Neurogastroenterol. Motil.* **21,** 551–558, e14–e15
25. Exley, R., Moroni, M., Sasdelli, F., Houlihan, L. M., Lukas, R. J., Sher, E., Zwart, R., and Bermudez, I. (2006) *J. Neurochem.* **98,** 876–885
26. Ben-Ami, H. C., Yassin, L., Farah, H., Michaeli, A., Eshel, M., and Treinin, M. (2005) *J. Biol. Chem.* **280,** 28053–28060
27. Cohen Ben-Ami, H., Biala, Y., Farah, H., Elishevitz, E., Battat, E., and Treinin, M. (2009) *Biochemistry* **48,** 12329–12336
28. Niesler, B., Walstab, J., Combrink, S., Möller, D., Kapeller, J., Rietdorf, J., Bönisch, H., Göthert, M., Rappold, G., and Brüss, M. (2007) *Mol. Pharmacol.* **72,** 8–17
29. Horton, R. M., Hunt, H. D., Ho, S. N., Pullen, J. K., and Pease, L. R. (1989) *Gene* **77,** 61–68
30. Walstab, J., Hammer, C., Bönisch, H., Rappold, G., and Niesler, B. (2008) *Pharmacogenet. Genomics* **18,** 793–802
31. Walstab, J., Combrink, S., Brüss, M., Göthert, M., Niesler, B., and Bönisch, H. (2007) *Anal. Biochem.* **368,** 185–192
32. Lo, W. Y., Botzolakis, E. J., Tang, X., and Macdonald, R. L. (2008) *J. Biol. Chem.* **283,** 29740–29752
33. Holbrook, J. D., Gill, C. H., Zebda, N., Spencer, J. P., Leyland, R., Rance, K. H., Trinh, H., Balmer, G., Kelly, F. M., Yusaf, S. P., Courtenay, N., Luck, J., Rhodes, A., Modha, S., Moore, S. E., Sanger, G. J., and Gunthorpe, M. J. (2009) *J. Neurochem.* **108,** 384–396
34. Karnovsky, A. M., Gotow, L. F., McKinley, D. D., Piechan, J. L., Ruble, C. L., Mills, C. J., Schellin, K. A., Slightom, J. L., Fitzgerald, L. R., Benjamin, C. W., and Roberds, S. L. (2003) *Gene* **319,** 137–148
35. Seredenina, T., Ferraro, T., Terstappen, G. C., Caricasole, A., and Roncarati, R. (2008) *Biosci. Rep.* **28,** 299–306
36. Thompson, A. J., and Lummis, S. C. (2007) *Expert Opin. Ther. Targets* **11,** 527–540
37. Monk, S. A., Williams, J. M., Hope, A. G., and Barnes, N. M. (2004) *Biochem. Pharmacol.* **68,** 1787–1796
38. Connolly, C. N., Krishek, B. J., McDonald, B. J., Smart, T. G., and Moss, S. J. (1996) *J. Biol. Chem.* **271,** 89–96
39. Castillo, M., Mulet, J., Gutiérrez, L. M., Ortiz, J. A., Castelán, F., Gerber, S., Sala, S., Sala, F., and Criado, M. (2005) *J. Biol. Chem.* **280,** 27062–27068
40. Shteingauz, A., Cohen, E., Biala, Y., and Treinin, M. (2009) *J. Cell Sci.* **122,** 807–812
41. Wang, Y., Yao, Y., Tang, X. Q., and Wang, Z. Z. (2009) *J. Neurosci.* **29,** 12625–12635
42. Alexander, J. K., Jefford, G., Criado, M., Sagher, D., and Green, W. N. (2007) in *Annual Meeting of the Society for Neuroscience, San Diego, November 3–7, 2007,* 575.3/K3, Society for Neuroscience, Washington, D. C.
43. Cooper, S. T., and Millar, N. S. (1997) *J. Neurochem.* **68,** 2140–2151
44. Walstab, J., Rappold, G., and Niesler, B. (2010) *Pharmacol. Ther.*, in press